Investigation to the deep center related properties of low temperature grown InPBi with Hall and photoluminescence

AIP Advances

Citation for the published paper:
Wang, P. ; Pan, W. ; Wang, K. et al. (2015) "Investigation to the deep center related properties of low temperature grown InPBi with Hall and photoluminescence". AIP Advances, vol. 5(12), pp. Article Number: 127104.

http://dx.doi.org/10.1063/1.4937412

AIP ADVANCES **5**, 127104 (2015)

Investigation to the deep center related properties of low temperature grown InPBi with Hall and photoluminescence

Peng Wang,[1,2] Wenwu Pan,[1,2] Kai Wang,[1,3] Xiaoyan Wu,[1,2] Li Yue,[1]
Qian Gong,[1] and Shumin Wang[1,4]
[1]*State Key Laboratory of Functional Materials for Informatics, Shanghai Institute of Microsystem and Information Technology, Chinese Academy of Science, Shanghai 200050, China*
[2]*School of Physics, University of Chinese Academy of Sciences, 19 Yuquan Road, Beijing, 100049, China*
[3]*National Laboratory for Infrared Physics, Chinese Academy of Sciences, 500 Yutian Road, Shanghai, 200083, China*
[4]*Department of Microtechnology and Nanoscience, Chalmers University of Technology, 41296 Gothenburg, Sweden*

(Received 5 September 2015; accepted 12 November 2015; published online 4 December 2015)

$InP_{1-x}Bi_x$ epilayers with bismuth (Bi) concentration x= 1.0% were grown on InP by gas source molecular beam epitaxy (GS-MBE) at low temperature (LT). Bi incorporation decreased the intrinsic free electron concentration of low temperature grown InP indicated by hall analysis. It is concluded that deep level center was introduced by Bi. Influence of Si doping on the $InP_{1-x}Bi_x$ films Photoluminescence (PL) was investigated. *N*-type doping in the $InP_{1-x}Bi_x$ epilayers was found to be effective at PL enhancement. Blue shift of InPBi PL emission wavelength was observed as the Si doping concentration increasing. Two independent peaks were fitted and their temperature dependence behavior was observed to be distinct obviously. Two individual radiative recombination processes were expected to be involved. © *2015 Author(s). All article content, except where otherwise noted, is licensed under a Creative Commons Attribution 3.0 Unported License.* [http://dx.doi.org/10.1063/1.4937412]

INTRODUCTION

III–V dilute bismuth (Bi) compound semiconductors have been attracting great attention for their promising potentials in the applications for near and mid infrared emitters and detectors.[1–4] Incorporation of Bi atoms at anion sites was proved to introduce distinct band gap reduction and enhanced spin-orbit (SO) splitting. In this way, more flexibility is achieved in band gap engineering for optoelectronic device application and the commonly fronted Auger recombination involving holes on the SO and the valence bands is expected to be suppressed effectively.[5] Moreover, temperature insensitive optical emission was detected in dilute InGaAsBi,[6] which is beneficial for telecom lasers. Bismuth, which has a much large atomic radius, introduces localized states close to the valance band maximum (VBM) and a valance band anti-crossing (VBAC) model has been utilized to describe influence of the Bi Incorporation on the band edges of the host III–V compound.[7] Much effort has been put into epitaxial growth and material properties of GaAsBi and GaSbBi. Light emission diodes (LEDs) and electrically injected lasers have been demonstrated using GaAsBi as an active layer.[8,9]

As an important material candidate for optoelectronic devices, group III phosphides have been extensively researched for decades.[10,11] Structural properties of Bi-bearing semiconductor alloys including InPBi, InAsBi and InSbBi have been theoretically investigated by Berding *et al*. and InPBi was found to be the most difficult to synthesize.[12] Besides the remarkable band gap shrink, Bi incorporation into InP is also expected to suppress above-mentioned Auger recombination and inter valance band absorption (IVBA) processes.[6] Early researches have been focused on the isoelectronic impurity state of InP:Bi at a doping level.[13,14] We have demonstrated the first successful fabrication of InPBi single crystals with Bi composition far beyond the theoretically predicted solubility limit and InGaPBi lattice matching with InP by gas source molecular beam epitaxy (GS-MBE)[15,16] and found 56 meV/Bi% reduction of band gap from optical absorption. It is worth noting that broad and strong photoluminescence (PL) signal is observed at room temperature with emission energy centered around 0.9 eV which is significantly lower than the measured InPBi band gap. Deep level radiative recombination centers introduced by Bi incorporation are supposed to be responsible for this PL emission. It is significant to figure out more properties of the deep level centers to understand the nature of InPBi.

In this work, InPBi single crystals with Bi component up to 1.0% were grown at low temperature on SI InP substrates by GS-MBE. Properties of the Bi related deep level center were investigated by analyzing Hall result of as grown InPBi and PL spectra of Si doped *n*-type InPBi. The compensation effect of Bi to the background free electron concentration was intensified at low temperature, which confirmed the fact that Bi incorporation has introduced deep level centers instead of shallow ones. *N*-type doping in the InPBi epilayers revealed to be productive at Photoluminescence wavelength blue-shift and intensity enhancement of the InPBi films. The radiative recombination process of LT grown InPBi was identified to be conduction band related. Temperature dependence behavior of LT grown InPBi PL emission was discussed.

EXPERIMENT

$InP_{0.99}Bi_{0.01}$ samples were grown on semi-insulating InP (100) substrates using a VG V90 GS-MBE. The InP substrates were first deoxidized at 480°C. As to InPBi growth, the substrate temperature was decreased significantly to 300°C for efficient Bi incorporation. All the growth temperatures were measured by a thermocouple (TC). Samples with in-situ *n*-type doping (Si for *n*-type doping) of varied electron concentrations were designed. The thickness of the InPBi epi-layer was fixed at around 360 nm. A reference InP sample was prepared under the same growth condition for comparison.

In terms of material characterization, Hall measures were first carried out in a van der Pauw geometry. The structural qualities were characterized by a Philips X'pert MRD high-resolution x-ray diffractometer (HRXRD) equipped with a four-crystal Ge (220) monochromator using Cu $K\alpha 1$ X-ray. The diffraction of (004) planes was measured using ω-2θ scans. Photoluminescence (PL) spectra were measured with a Nicolet Magna 860 Fourier transform infrared (FTIR) spectrometer from Thermo Fisher Scientific Inc. A liquid-nitrogen cooled InSb detector and a CaF_2 beam splitter were equipped. Samples were excited by a diode-pumped solid state (DPSS) laser ($\lambda = 532$nm) and the double modulation mode was used to eliminate the mid-infrared background radiation over 2μm. Low temperature PL measurements were carried out by mounting samples into a continuous-flow helium cryostat, and a Lake Shore 330 temperature controller was used to adjust the temperature form 20 to 270 K.

RESULTS AND DISCUSSIONS

Table I shows carrier concentration and electron mobility of InPBi samples as well as the reference InP sample. A free electron concentration of 3.3×10^{18} cm^{-3} was observed from the InP reference sample at RT. Use of a low growth temperature will introduce extra antisite defects P_{In} which

TABLE I. Summary of Hall measurement results.

List	Samples	Doping type	carrier concentration (cm^{-3})	Mobility (cm^2 /V• s)
1	InP reference	/	-3.3×10^{18} -3.2×10^{18} (77K)	1000 940 (77K)
2	InPBi	/	-1.2×10^{18} -0.84×10^{18} (77K)	1100 837 (77K)
3	InPBi	*n* (Si)	-3.0×10^{18}	1100
4	InPBi	*n* (Si)	-5.0×10^{18}	1000
5	InPBi	*n* (Si)	-1.0×10^{19}	890

act as donor centers, leading to the *n*-type conduction.[17] Auto-ionization of the first ionization state of P_{In}, above the conduction band minimum (CBM), generates free electrons in LT grown InP. Undoped InPBi sample also reveals to be *n*-type but with an electron concentration of 1.2×10^{18} cm^{-3}, about one third of that found in the InP reference sample. Two possible reasons were expected for the decrease of free carrier concentration. First, Bi incorporation has introduced additional acceptor-like centers compensating the *n*-type background of the LT grown InP. Second, the stochiometry of the LT grown InP is improved by Bi incorporation leading to a significant reduction of antisite defects P_{In}. As auto-ionization process is temperature insensitive, free electron concentration generated from P_{In} is also expected to be less temperature dependent, which was revealed by the 77K Hall test of LT grown InP shown in Table I. A significant decrease of the free electron concentration was observed in InPBi at 77K as shown in Table I and this indicates the second assumption indefensible. Two compensating mechanisms of the free electrons are anticipated: neutralization by shallow level acceptor centers and bound of free electrons by Bi induced deep level centers. In the former case, free hole concentration decreases at 77K compared with that at RT. The corresponding compensation effect would be enhanced at RT, which is opposite to the experimental findings. This can be an indirect evidence for the existence of deep level centers introduced by Bi incorporation. The ability of deep levels to bound free electrons decreases with increasing temperature, leading to less compensation at RT than at 77K. Detailed temperature dependent Hall test result also supports the above standpoint.

Electron mobility of InPBi is 10% higher than that of InP at RT, possibly due to the lower electron density in InPBi thus the reduction of the electron-electron scattering. The electron mobility of the LT InP decreases by 6% while the electron concentration remains almost the same from RT to 77K, indicating that the ionized impurity scattering can be important in this temperature range. This is reasonable since the density of such auto-ionized impurities is on the order of 10^{18} cm^{-3}. However, the electron mobility of InPBi decreases by 24% from RT to 77K. Extra scattering mechanism due to the Bi incorporation must be functioning. One possibility is the alloy scattering as a result of non-uniformity induced by Bi clusters. Si doping in InPBi has increased the electron concentration from 3.0×10^{18} cm^{-3} up to 1.0×10^{19} cm^{-3} and electron mobility decreased by 19% meanwhile due to the enhancement of electron-electron scattering. We have tried Be doping in InPBi but fail to achieve *p*-type in spite of that it leads to *p*-type conduction in the LT InP reference sample. We suspect that Be tends to form complex with Bi and lose its acceptor nature.

Crystal quality of InPBi epi-layers was examined by HRXRD with results shown in Figure 1. Besides sharp peaks of the InP (100) substrate, all samples show obvious InPBi diffraction peaks indicating the strict growth orientation inheriting form the InP substrate. All the InPBi samples have positive mismatching with the InP substrate demonstrating the extended lattice constant by Bi incorporation. The peak position is indicated by the dashed line and the full width at a half maximum (FWHM) are nearly unchanged with increasing Si doping concentration, implying little influence of the Si doping on the structural quality of InPBi. It is worth to mention that little strain relaxation has taken place because of the small mismatch between epi-layers and substrates.

Doping of InPBi provides us more access to perspective into the nature of InPBi PL emission. Figure 2 shows RT PL spectra of *n*-type doped InPBi films. A broad asymmetric emission band centered around 0.9 eV is observed for all InPBi samples. Peak blue-shift introduced by *n*-type doping is shown with the dash line arrow. PL intensity of PL emission peaks is enhanced by *n*-type doping up to 5×10^{18} cm $^{-3}$ and further doping up to 1×10^{19} cm^{-3} inverts the tendency.

In *n*-type semiconductors, the radiative recombination rate is proportional to free electron concentration *n* when the recombination process is related to the conduction band. Thus, higher radiative recombination efficiency is expected as Si doping concentration increasing. PL emission intensity is plotted as a function of electron concentration of InPBi in the inset of Figure 3, in which linear dependence followed with significant reduction behavior was consistent with above discussion. The PL intensity reduction might be a result of free carrier absorption or Si doping introduced non-radiative recombination centers. Figure 3 shows PL peak energy as a function of Si doping concentration by black squares. An approximate linear blue-shift of peak energy is observed, which can be ascribed to Burstein-Moss effect.[18] N-type doping lifts the electron Fermi level in the conduction band increasing the electrons filling level and results in increasing of photon energy in radiative recombination. We

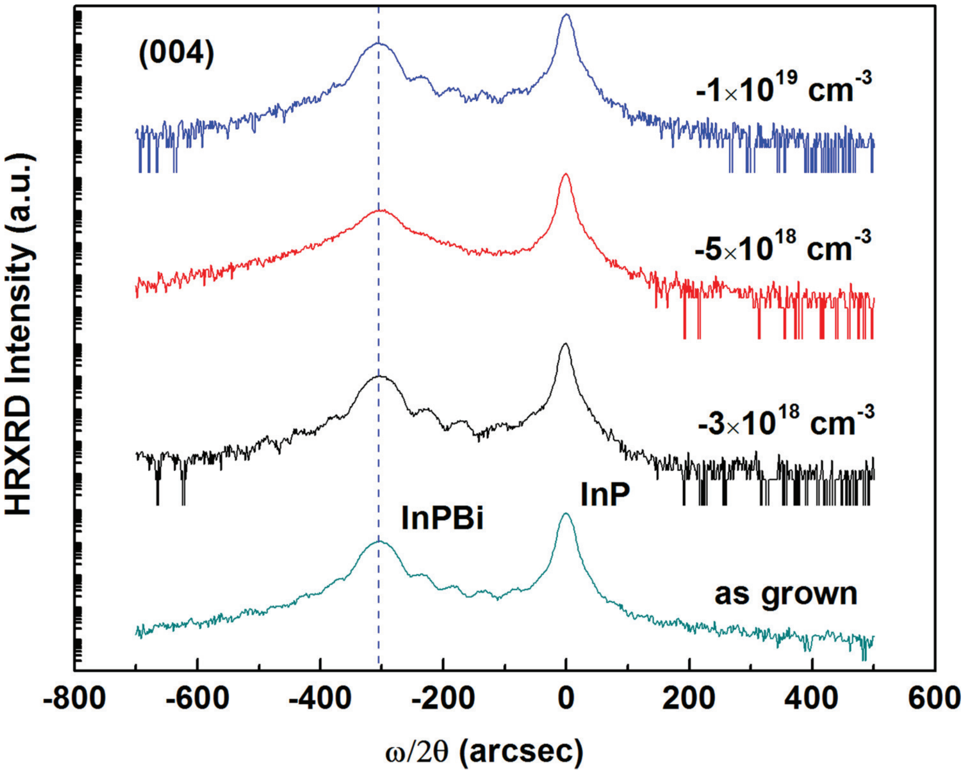

FIG. 1. HRXRD (004) rocking curves of InPBi with varied n-type doping concentrations.

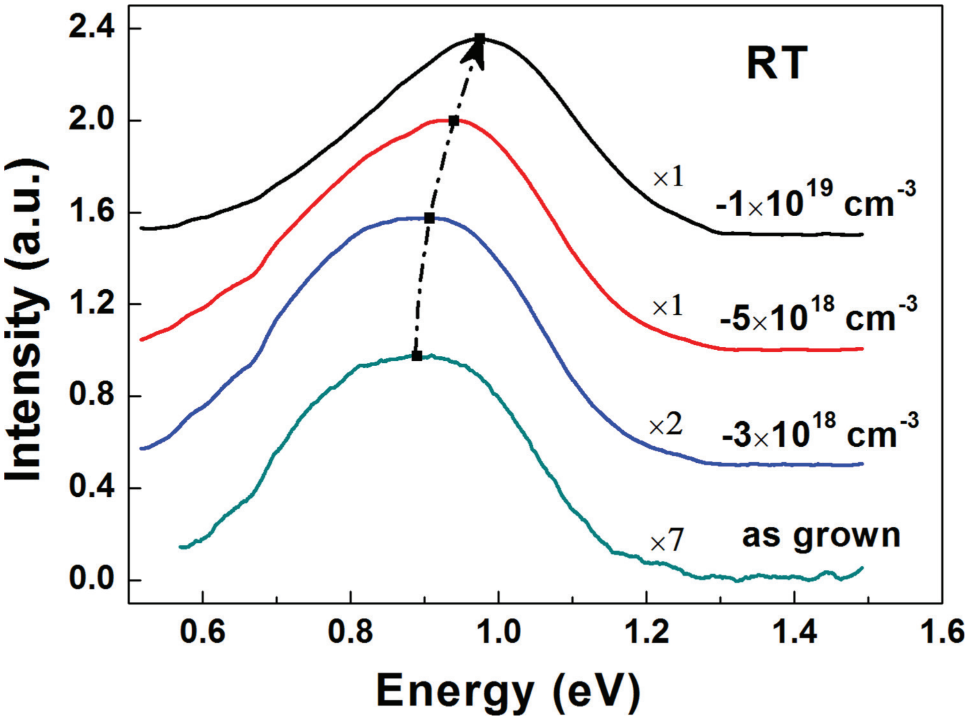

FIG. 2. RT PL spectra of as grown and Si doped InPBi samples.

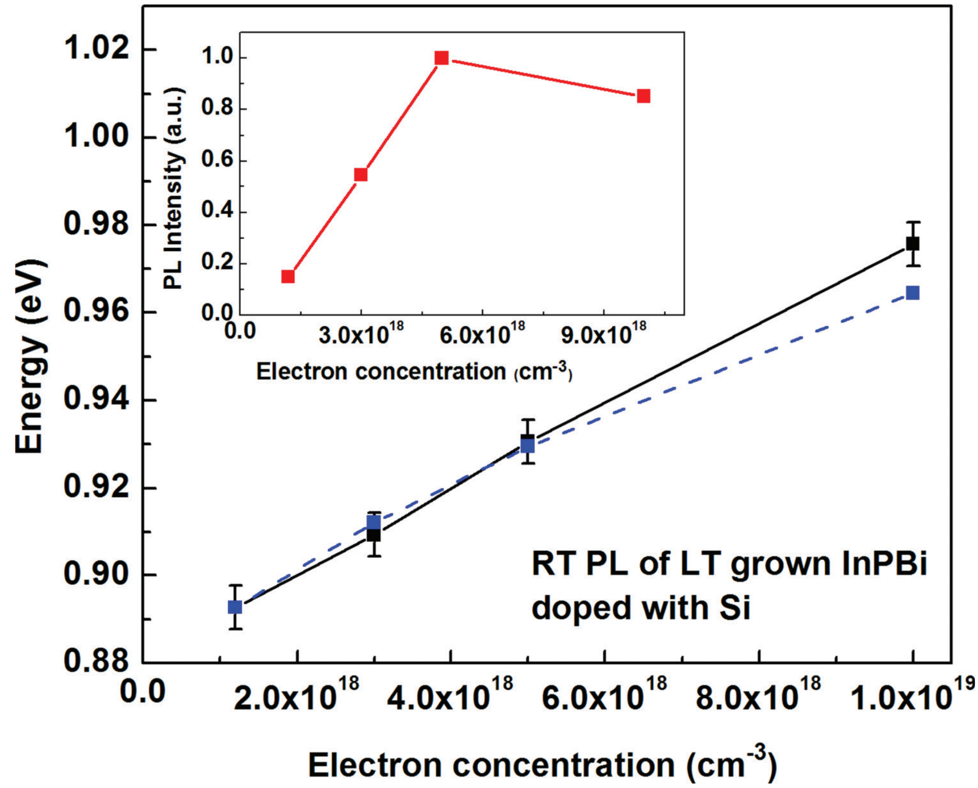

FIG. 3. PL peak energy and intensity (inset) as a function of Si doping concentration. The black square dots are measured data while the blue dots are the estimated results.

have reported that PL emission of InPBi is related to the Bi induced deep level center.[19] Our preliminary result of deep level transient spectroscopy (DLTS) test indicates existence of the Bi induced acceptor like deep level center (not shown here). From this point of view, we can ascribe PL emission of InPBi to radiative recombination between electrons in conduction band and holes bounded at the deep level introduced by Bi incorporation.

Magnitude of the Burstein-Moss shift (Δ_{BM}), under free-electron theory, is defined as

$$\Delta_{BM} = \frac{\hbar^2}{2m^*}(3\pi^2 n_e)^{2/3}.$$

Δ_{BM} is inversely proportional to reduced effective mass m^*, which can be derived from valance and conduction band effective, m_v^* and m_c^*, according to $1/m^* = 1/m_v^* + 1/m_c^*$, and proportional to $(n_e)^{2/3}$, where n_e is the electron concentration. In general, Burstein-Moss shift refers to band to band transition. As the effective mass of hole m_v^* is much larger than the effective electron mass m_c^*, Δ_{BM} most comes from electrons filling of conduction band. Therefore, we have still carried out the calculation using parameters of InP, which was presented by blue squares and the dash line in Figure 3. A good fitting of the simulation to the experiment results is revealed within the marginal error, confirming the fact that the PL emission blue-shift originates from the conduction band filling effect. A relatively distinct discrepancy is revealed for the InPBi sample with electron concentration up to 1×10^{19} cm^{-3}. One possible reason is difference in effective mass between InP and InPBi.

Band gap renormalization, which is considered as a result of mutual exchange and Coulomb interactions between the added free electrons and electron-impurity scattering, was also taken into account.[20] Specific behavior of band-gap renormalization was the low energy side widening of PL spectra with electron concentration increasing, as shown in Figure 2. *N*-type doping introduces band tailing below the conduction band minimum (CBM), which result in radiative recombination spreading to the low-energy side.[21]

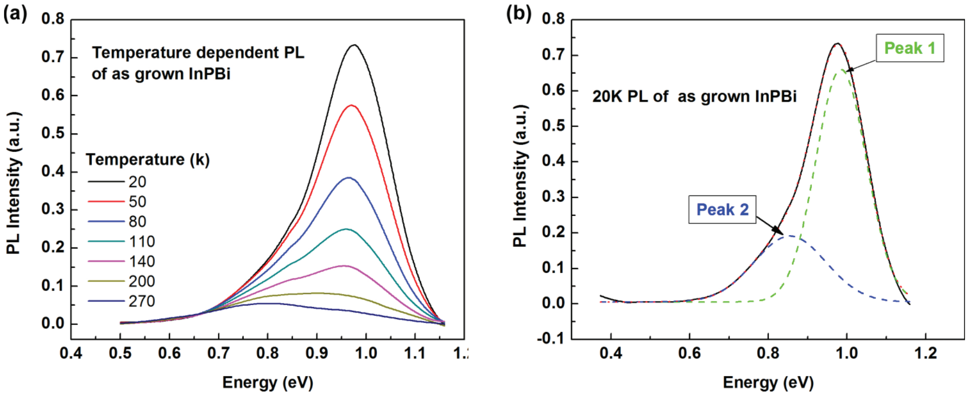

FIG. 4. (a) temperature dependent PL spectra of as grown InPBi sample. (b) double peaks fitting of 20K PL spectra.

Temperature dependent PL was detected for all InPBi samples and PL spectra of the undoped InPBi sample are shown Figure 4(a). As can be seen, PL intensity increases dramatically with decreasing temperature and the PL shape changes simultaneously. The PL spectra reveal obviously asymmetric and two independent peaks and are fitted using Gaussian function as shown in Figure 4(b). Temperature dependent behavior of the two fitted peaks is anticipated to be distinct from each other. We have extracted the variation trend as a function of temperature for both peaks respectively. In terms of peak energy, two distinct temperature dependent behaviors are observed as shown in Fig. 5(a). As temperature increasing, peak energy red shifted consistently for peak 1. Semi-empirical Varshni's formula with form as

$$E_g = E_g^0 - \frac{\alpha T^2}{T + \beta}$$

in which E_g^0 is the band-gap energy at 0 K, has indicated that bandgap energy is reduced with temperature increasing as a result of crystal lattice thermal expansion, which leads to the red shift of peak 1. In spite of the fact that PL emission did not originate from band-to-band recombination, we still make a fitting using the same form of Varshni's formula with E_Δ^0 replacing E_g^0 plotted with the blue dash line in Figure 5(a). Experiment result was mainly matched to the fitting curve which can be regarded as an evidence for uniform band-gap shrinkage with temperature increasing. Fitting result of the parameters for Varshni's formula were listed: $E_\Delta^0 = 0.852\text{eV}$, $\alpha = 6.73 \times 10^{-4}$, $\beta = 611$. The fitted parameters have great difference with that of InP, which is due to basic properties variation of InPBi compared with InP. Temperature dependent trend of peak 2 revealed to be quite different from peak 1 and no notable shift was observed. Temperature dependence of emission intensity for both peaks was also presented in figure 5(b). Emission intensity of peak 2 dropped more dramatically than that

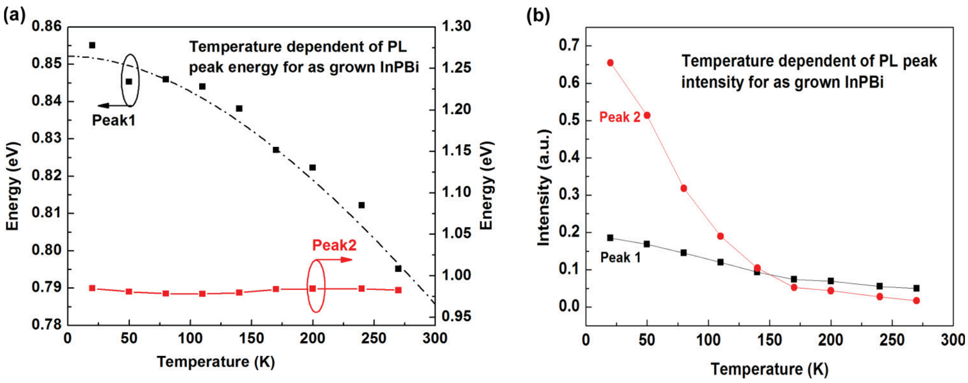

FIG. 5. Temperature dependence of emission energy (a) and intensity (b) for as grown InPBi sample.

of peak 1 and evolved from the stronger to the slightly weaker one as temperature increasing. Distinct temperature dependent behavior of two emissions indicated that two different radiative recombination processes were involved in the PL of LT grown InPBi. The increasing nonradiative recombination transition rate as temperature rising weaken the peak 2 related radiative transition more dramatically as shown in figure 5(b). We have carried out cross-sectional scanning tunneling microscopy (X-STM) of Bi atoms in InPBi to investigate Bi distribution at lattice (not shown here). Bi cluster was observed besides Bi uniform incorporation into the zinc-blende lattice. The distribution nonuniformity of Bi incorporation might be the origination of non-monolithic radiative recombination processes in LT grown InPBi. We have also analyzed the temperature dependent spectra of Si doped InPBi, quite different evolution behavior is observed which will be discussed in detail elsewhere.

As a summary, InPBi films with 1% Bi concentration were grown by GSMBE at LT. Bi incorporation has introduced additional deep level acceptor centers trapping free electrons and compensating the background n-type conductivity of low temperature grown InP, which was indicated by hall analysis. *N*-type doping with Si impurity into InPBi films with varied doping concentration was carried out. PL test results indicated that *n*-type doping in the InPBi films lead to emission wavelength blue-shift and dramatic enhancement of the emission intensity, which can be explained with conduction band filling effect. The radiative recombination process was confirmed to be conduction band related. LT PL spectrum of as grown InPBi revealed two individual emission peaks with distinct temperature dependent behavior. Two different radiative recombination transition processes were expected to be involved.

ACKNOWLEDGEMENTS

The authors wish to acknowledge the financial support of the National Basic Research Program of China (Grant No. 2014CB643902), the Key Program of Natural Science Foundation of China (Grant No. 61334004), the Natural Science Foundation of China (Grant No. 61404152), the “Strategic Priority Research Program” of the Chinese Academy of Sciences (Grant No. XDA5-1), the foundation of National Laboratory for Infrared Physics, the Key Research Program of the Chinese Academy of Sciences (Grant No. KGZD-EW-804) and the Creative Research Group Project of Natural Science Foundation of China (Grant No. 61321492).

[1] K. O. a. H. OKAMOTO, “New Semiconductors Alloy GaAsBi Grown by Metal Organic Vapor Phase Epitaxy,” Jpn. J. Appl. Phys **37** (1998) (Part 2, No. 11A).

[2] B. Fluegel, S. F., A. Mascarenhas, S. Tixier, E. C. Young, and T. Tiedje, “Giant Spin-Orbit Bowing in $GaAs_{1-x}Bi_x$,” PHYSICAL REVIEW LETTERS **97**, 067205 (2006).

[3] Heather Jacobsen, B. P., Thomas F. Kuech, and Dane Morgan, “Ab initio study of the strain dependent thermodynamics of Bi doping in GaAs,” Physical Review B **86**, 085207 (2012).

[4] M. K. Rajpalke, W. M. L., M. Birkett, K. M. Yu, D. O. Scanlon, J. Buckeridge, T. S. Jones, M. J. Ashwin, and T. D. Veal, “Growth and properties of GaSbBi alloys,” Applied Physics Letters **103**, 142106 (2013).

[5] Ville Virkkala, V. H., Filip Tuomisto, and Martti J. Puska, “Modeling Bi-induced changes in the electronic structure of $GaAs_{1-x}Bi_x$ alloys,” Physical Review B **88**, 235201 (2013).

[6] S. R. Jin and Sweeney, “InGaAsBi alloys on InP for efficient near- and mid- infrared light emitting devices,” Journal of Applied Physics **114**, 213103 (2013).

[7] J. P. Petropoulos, Y. Z., and J. M. O. Zide, “Optical and electrical characterization of InGaBiAs for use as a mid-infrared optoelectronic material,” Appl. Phys. Lett. **99**, 031110 (2011).

[8] P. Ludewig, N. K., N. Hossain, S. Reinhard, L. Nattermann, I. P. Marko, S. R. Jin, K. Hild, S. Chatterjee, W. Stolz, S. J. Sweeney, and K. Volz1, “Electrical injection Ga(AsBi)/(AlGa)As single quantum well laser,” Applied Physics Letters **102**, 242115 (2013).

[9] N. Hossain, I. P. M., S. R. Jin, 1 K. Hild, S. J. Sweeney, R. B. Lewis, D. A. Beaton, and T. Tiedje, “Recombination mechanisms and band alignment of $GaAs_{1-x}Bi_x$/GaAs light emitting diodes,” Applied Physics Letters **100**, 051105 (2012).

[10] K Streubel, N Linder, R Wirth, and A Jaeger, “High brightness AlGaInP light-emitting diodes,” IEEE J Sel Topics in Quan Electron **8**, 321–332 (2002).

[11] M Yamamoto, N Yamamoto, and J Nakano, “MOVPE growth of strained InAsP/InGaAsP quantum-well structures for low-threshold 1.3-μm lasers,” IEEE J Quan Electron **30**, 554–561 (1994).

[12] M. A. Berding, A. Sher, A.B. Chen, and W. E Miller, “Structural properties of bismuth bearing semiconductor alloys,” Journal of Applied Physics **63**, 107 (1988).

[13] P.J. Dean, A. M. W., E.W. Williams, and M.G. Astles, “The isoelectronic trap bismuth in indium phosphide,” Soild State Communications **9**, 18 (1971).

[14] S. Riihle, R. Meek, N. Stath, J. U. Fischbach, I. Strottner, K. W. Benz, and M. Pilkuhn, “Isoelectronic impurity states in direct-gap III-V compounds: The case of InP:Bi,” Physical Review B **18**, 12 (1978).

[15] Yi Gu, Kai Wang, Haifei Zhou, Yaoyao Li, Chunfang Cao, Liyao Zhang, Yonggang Zhang, Qian Gong, and Shumin Wang, "Structural and optical characterizations of InPBi thin films grown by molecular beam epitaxy," Nanoscale Research Letters **9**, 24 (2014).

[16] K Wang, P Wang, W W Pan, X Y Wu, L Yue, Q Gong, and S M Wang, "Growth of semiconductor alloy InGaPBi on InP by molecular beam epitaxy," Semicond. Sci. Technol. **30**, 094006 (2015).

[17] B. W. Liang, P. Z. L., D. W. Shih, and C. W. Tu, "Electrical properties of InP grown by gas-source molecular beam epitaxy at Low temperature," Appl. Phys. Lett. **60**, 2014 (1992).

[18] H. P. D. Schenk, S. I. B., A. Berezin, A. Schön, E. Cheifetz, S. Khatsevich, and D. H. Rich, "Band gap narrowing and radiative efficiency of silicon doped GaN," Journal of Applied Physics **103**, 103502 (2008).

[19] K. Wang, Y. Gu, H. F. Zhou, L. Y. Zhang, C. Z. Kang, M. J. Wu, W. W. Pan, P. F. Lu, Q. Gong, and S. M. Wang, "InPBi single crystals grown by molecular beam epitaxy," Scientific Reports **4**, 5447 (2014).

[20] H. Q. Zheng, K. R., S. F. Yoon, and G. I. Ng, "Electrical and optical properties of Si-doped InP grown by solid sourcemolecular beam epitaxy using a valved phosphorus cracker cell," Journal of Applied Physics **87**, 11 (2000).

[21] Nam-Young Lee, Kyu-Jang Lee, Chul Lee, Jae-Eun Kim, Hae Young Peak, Dong–Hwa Kwak, Hee-chul Lee, and H. Lim, "Determination of conduction band tail and Fermi energy of heavily Si-doped GaAs by room-temperature photoluminescence," Journal of Applied Physics **78**, 5 (1995).